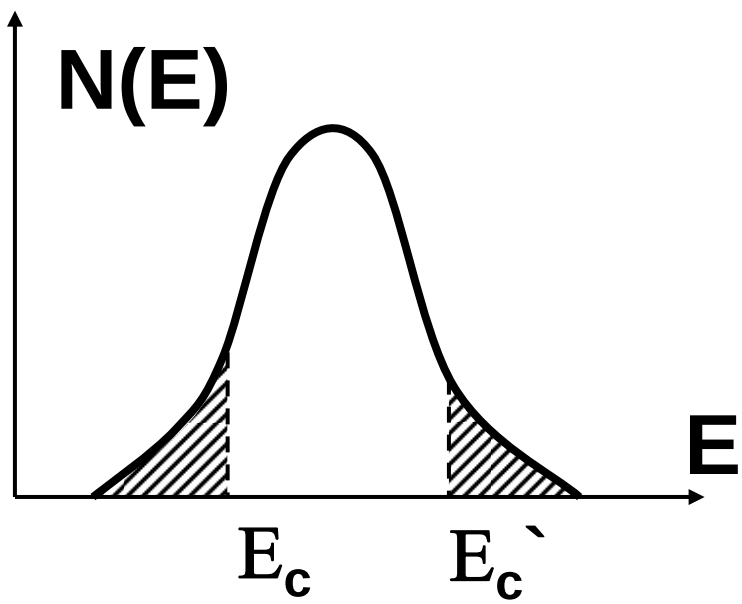

FIG.1 Density of band states in disordered solid. Dashed areas correspond to localized states and blank area means delocalized states. The boundary energies E_c and E'_c separating localized and extended states represent the mobility edges.

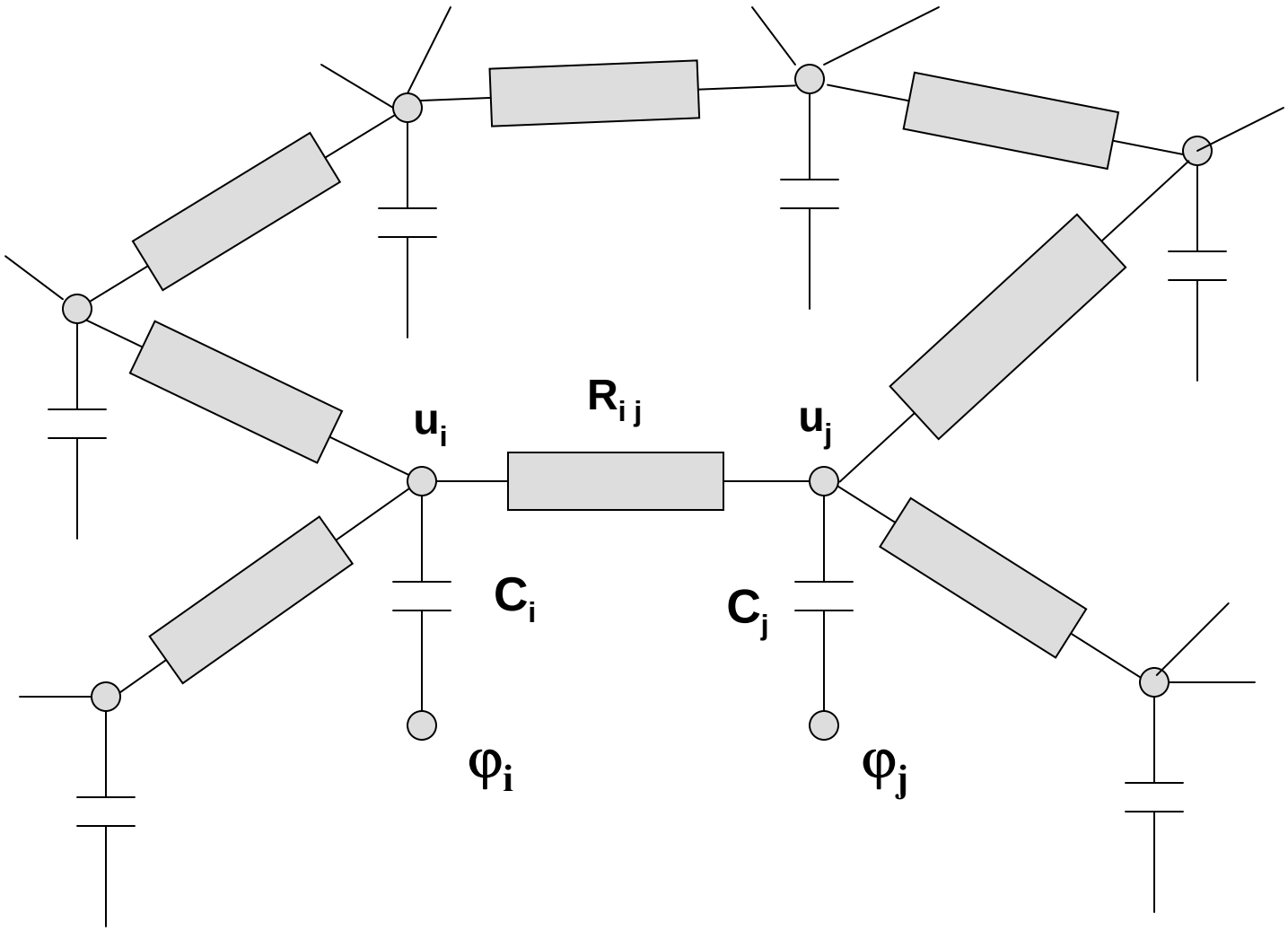

FIG.2 Equivalent electric circuit scheme for hopping network. The parameters are defined in the text.

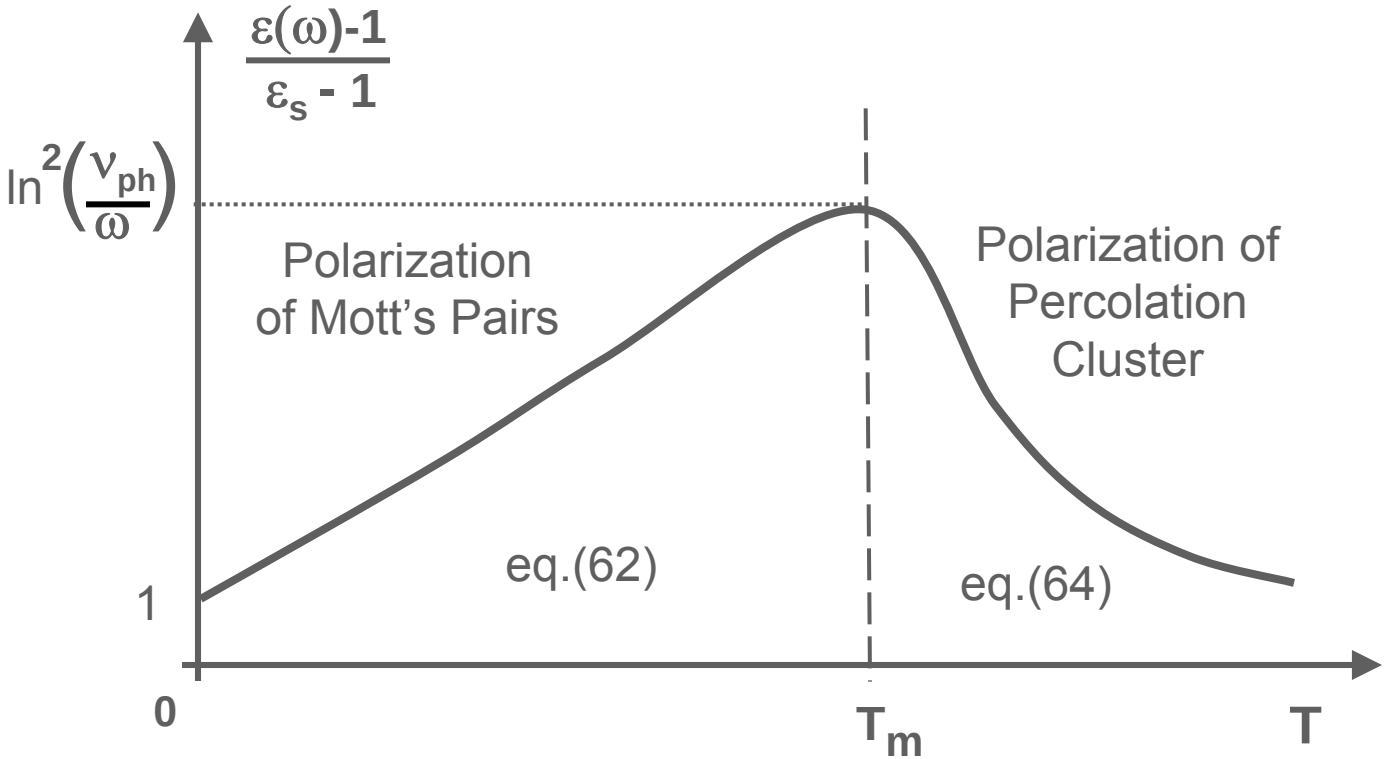

FIG. 3 The temperature dependence of dielectric constant for isotropic variable range hopping (*d* = 2,3) with characteristic maximum. Initial linear increase of dielectric constant is due to polarization of closely located states. The decrease at high temperature reflects the decrease of charge inhomogeneity in the conducting state due to the increase of charge mobility with increasing temperature. The position of the maximum depends on the frequency (Equation 4.65) (After Prigodin, V.N., Samukhin, A.N., and Epstein, A.J., *Synth. Met*., 141, 155, 2004. With permission.)

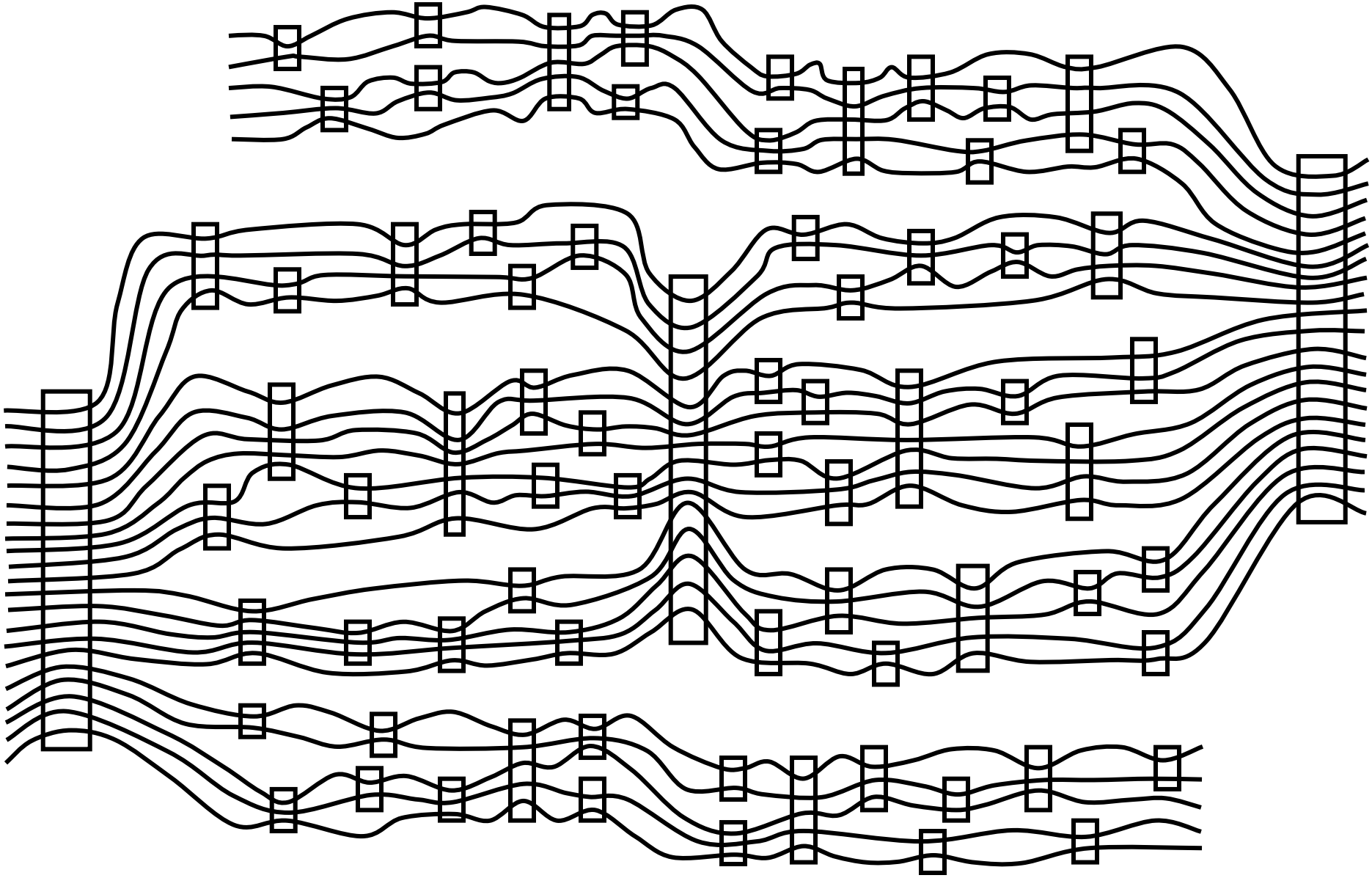

FIG.4 Schematic of chain fractal.

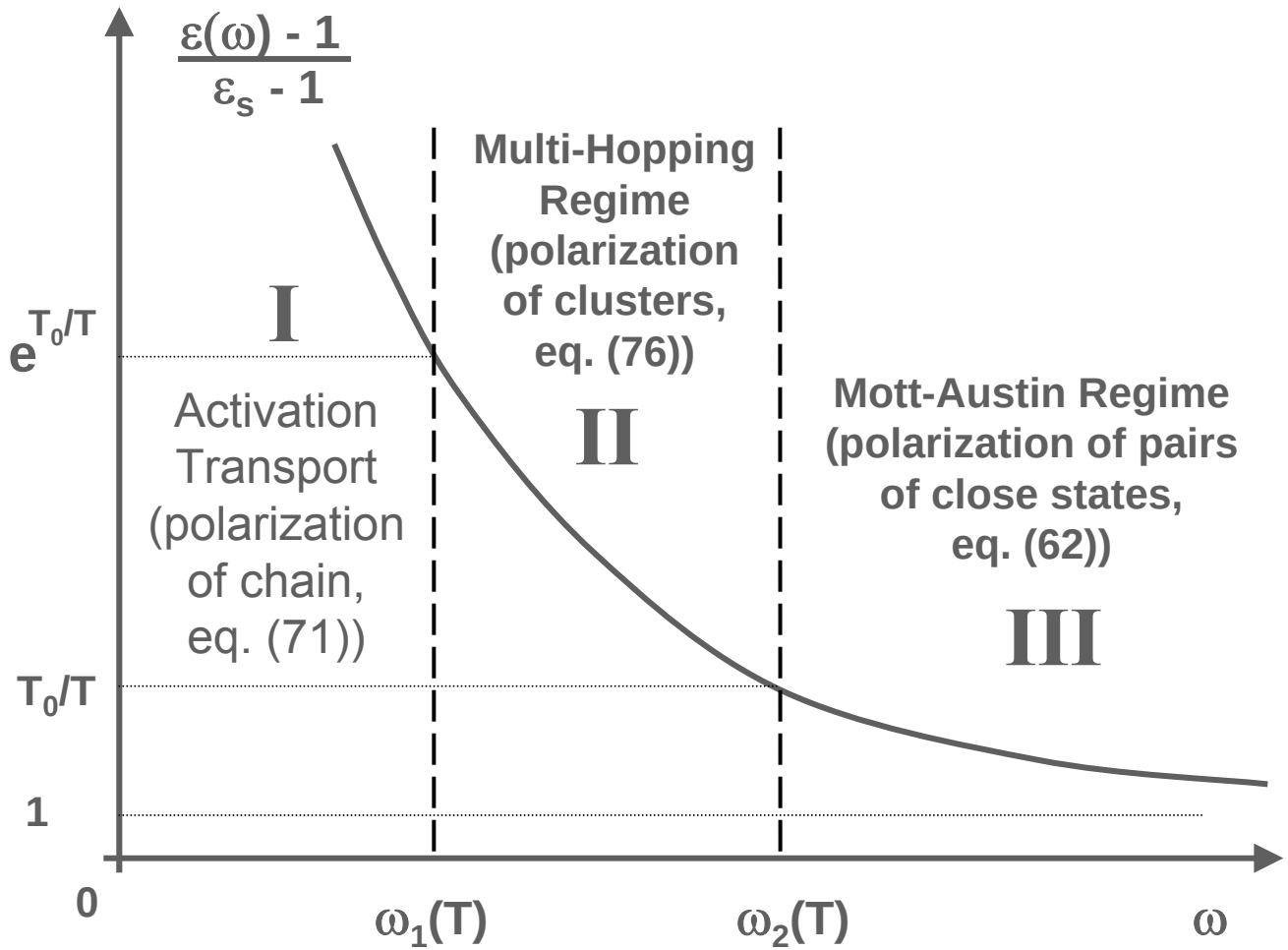

FIG.5 The frequency dependence of dielectric constant of 1D electronic system in the regime of variable range hopping. Three different regimes of ac-response can be easily identified.

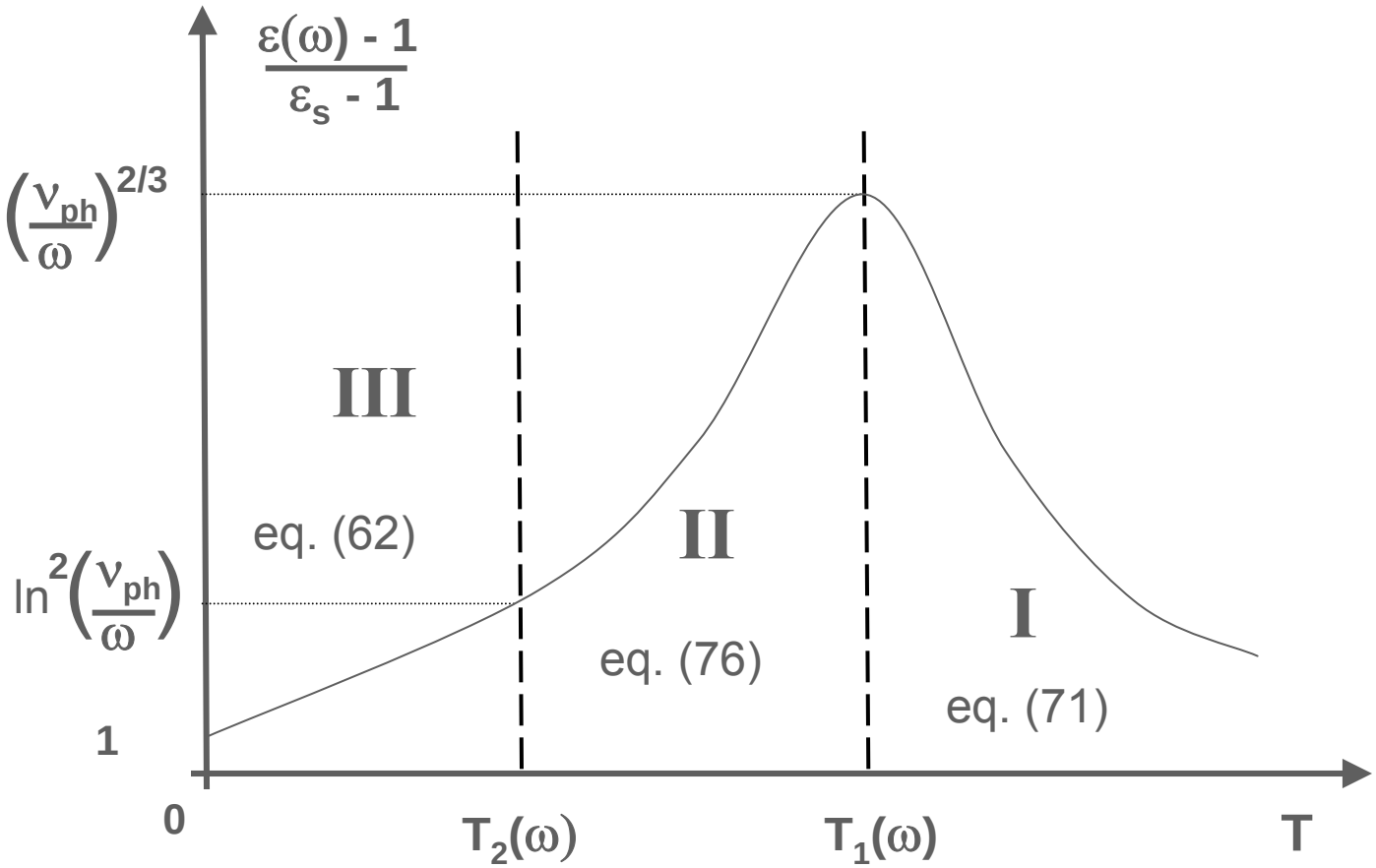

FIG.6 The temperature dependence of dielectric constant for the 1D system disordered chain. The initial linear increase describing the polarization of close states transforms into a strong exponential temperature dependence describing the polarization of extended chain cluster whose size is controlled by interchain hopping. At high temperatures the dielectric constant asymptotes to a constant value.

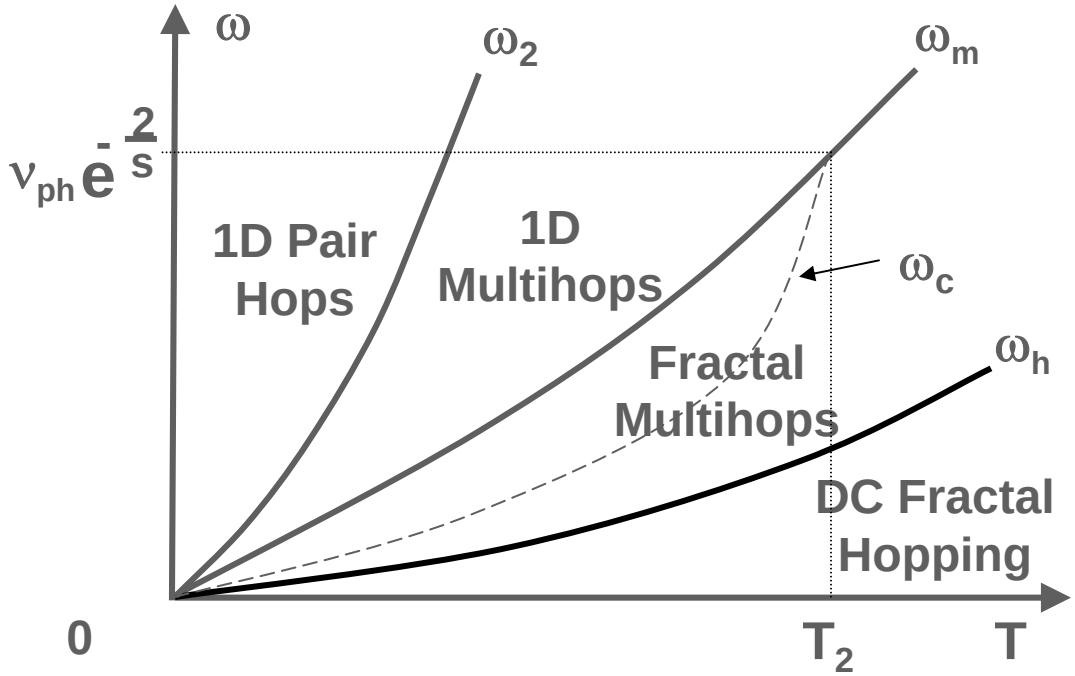

FIG.7 The diagram of hopping regimes for the fractal chain. The different boundary frequencies are defined in the text by Equations 4.77, 4.86, 4.95, and 4.85).

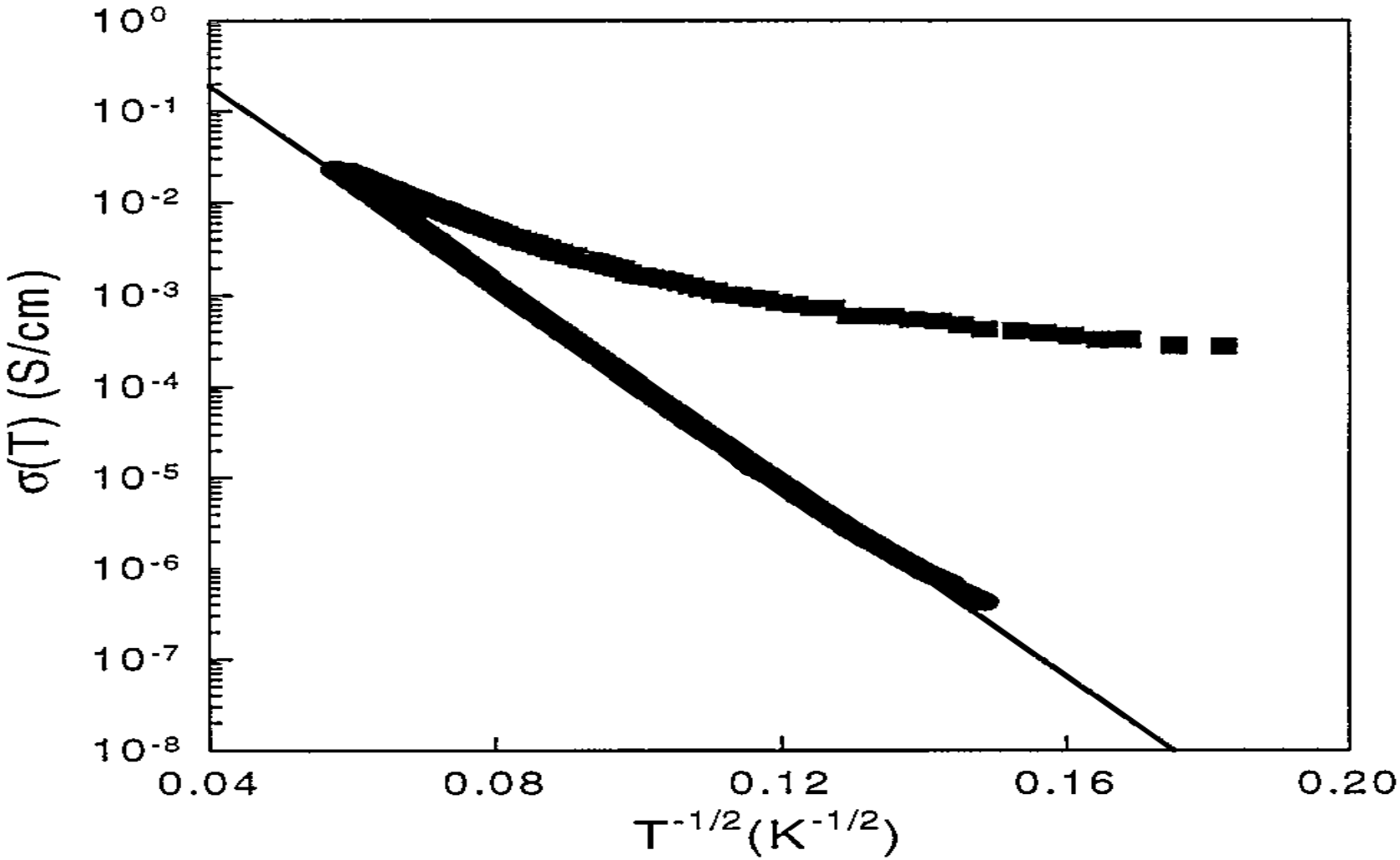

FIG.8 The temperature dependence of dc-conductivity (•) and microwave conductivity at 6.5 GHz (■) of sulfonated polyaniline. (After Lee, W.-P., Du, G., Long, S.M., Epstein, A.J., Shimizu, S., Saitoh, T., and Uzawa, M., *Synth. Met*., 84, 807, 1997. With permission.) The σ_{dc} (T) closely follows the quasi-1D Mott's law. It is noted that caution must be taken to review a large range of conductivity variation in identification of the temperature dependence.

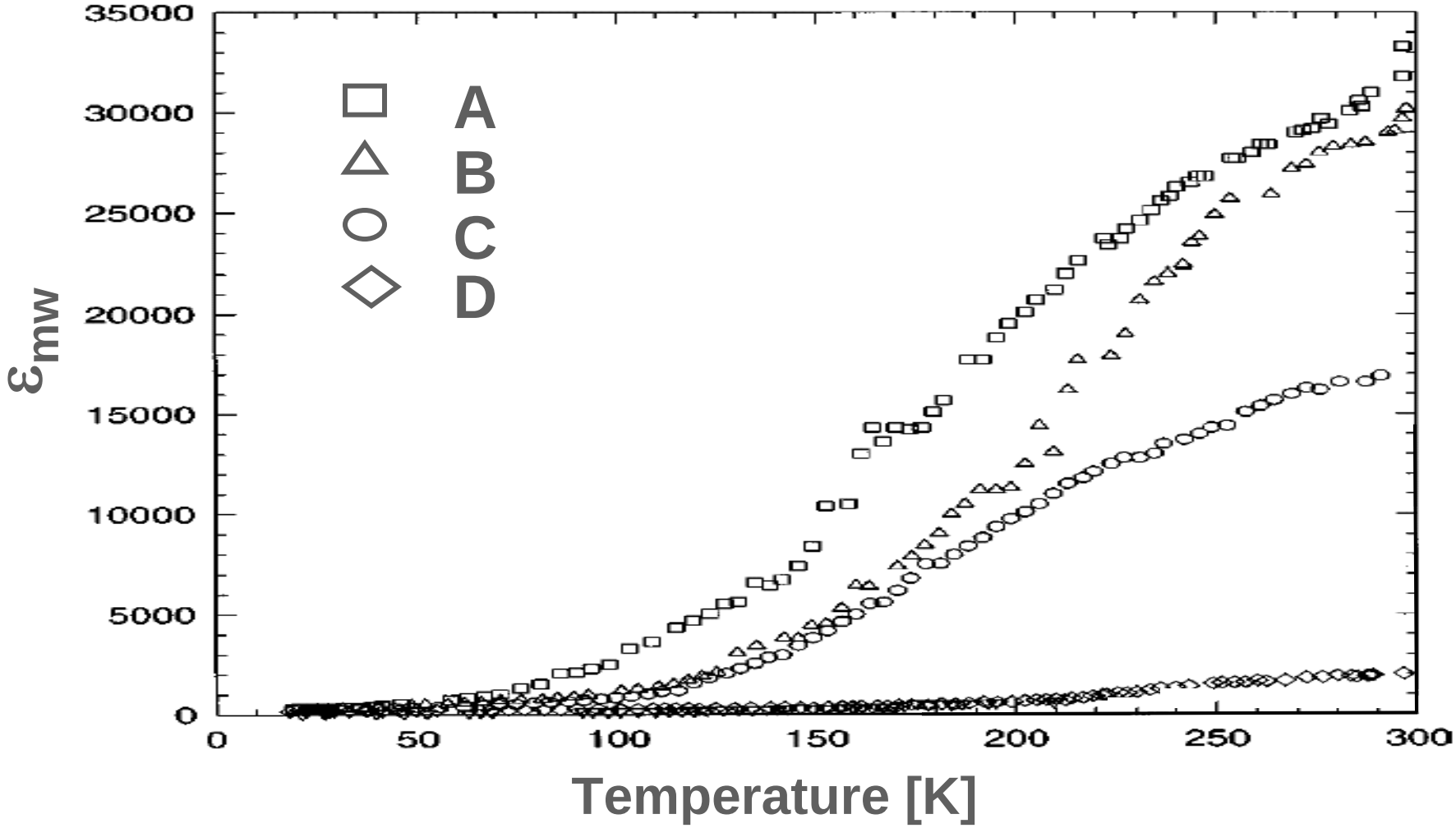

FIG.9 Temperature-dependent of microwave frequency (6.5 GHz) dielectric constant ε_{mw} (T) in the parallel direction for polyaniline films that have been stretched to provide partial orientation of the polymer chains. (After Joo, J., Long, S.M., Pouget, J.P., Oh, E.J., MacDiarmid, A.G., and Epstein, A.J., *Phys. Rev. B*, 57, 9567, 1998. With permission.) A and B are the most highly crystalline samples, and C and D are the least crystalline samples.

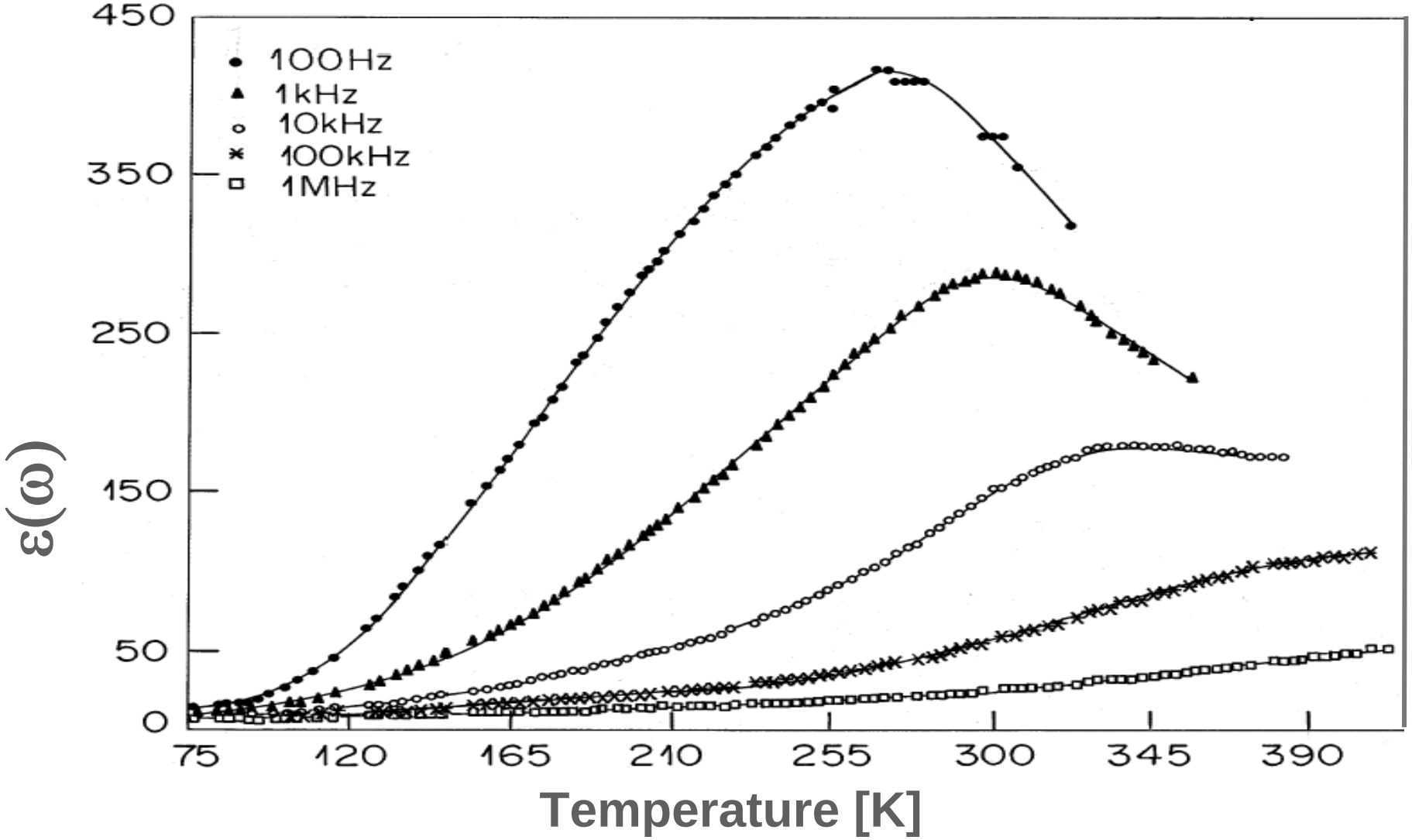

FIG.10 Dielectric constant plotted as a function of temperature for five fixed frequencies for doped polyaniline. (After Singh, R., Arora, V., Tandon, R.P., Mansingh, A., and Chandra, S., *Synth. Met*., 104, 137, 1999. With permission.)

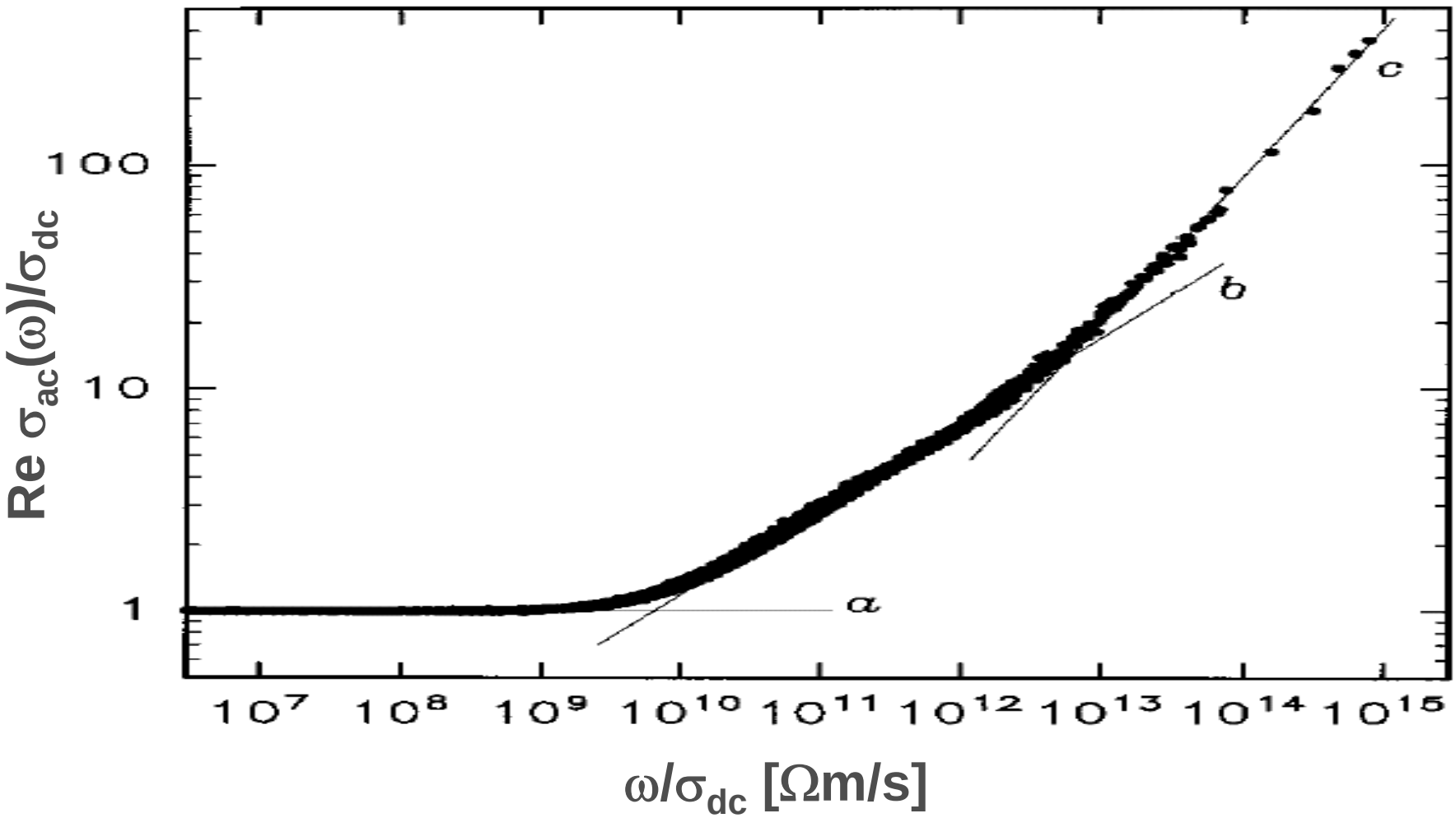

FIG.11 Scaled conductivity vs. scaled frequency for a conducting carbon-black (CB12) /nonconducting thermo-set polymer composite with carbon-black volume fraction *p* of 1×10^{-3} ($p = p_c/3$). The data taken at about 20 different temperatures between 300 and 4.2 K. (After Brom, H.B., Reedijk, J.A., Martens, H.C.F., Adriaanse, L.J., de Jongh, L.J., and Michels, M.A.J., *phys. stat. sol*. (b), 205, 103, 1998. With permission.) The three slopes are $\alpha = 0$ (dc-regime), $b = 0.4$ (quasi-fractal with $s = 0.8$), and $c = 0.7$ (pair hops).

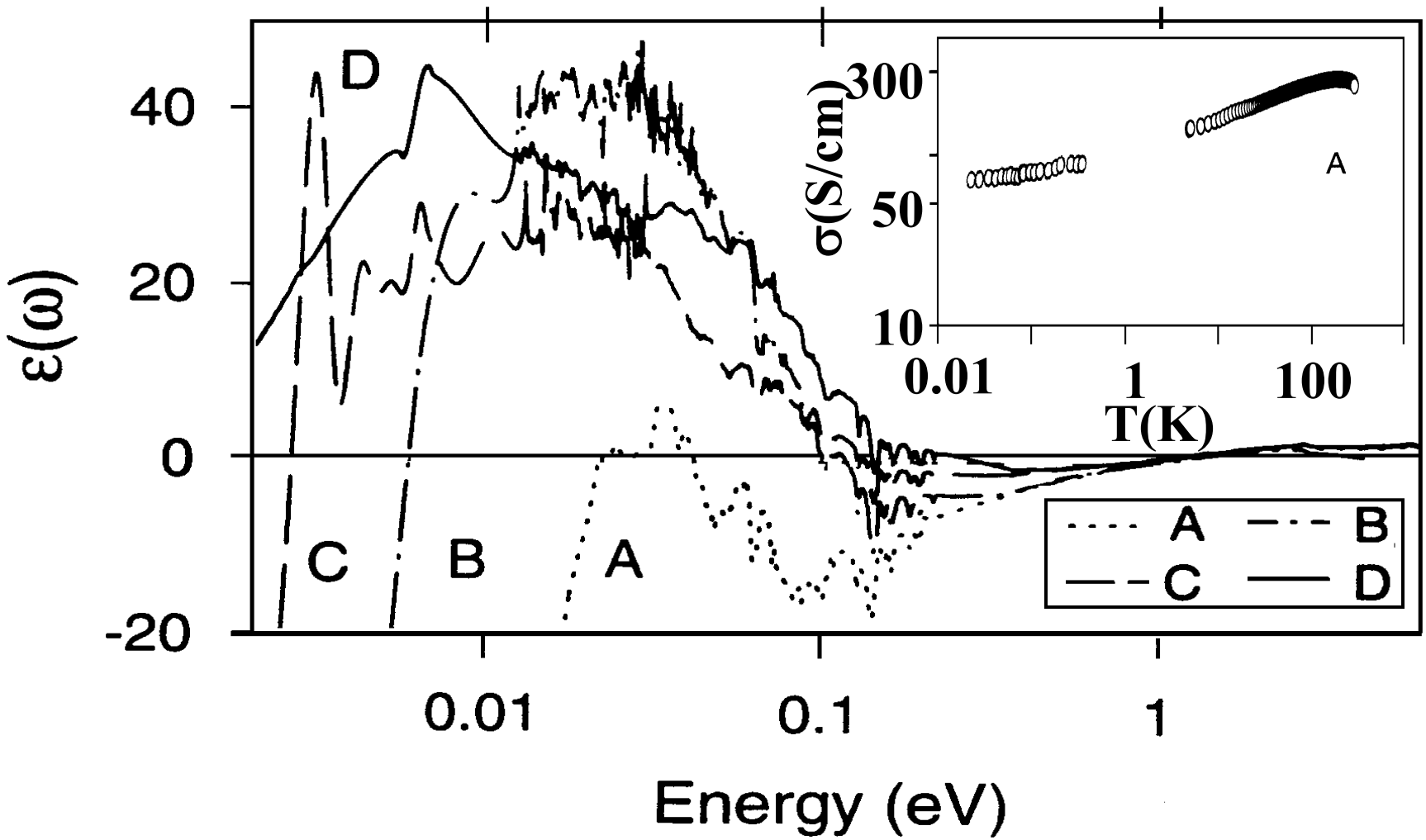

FIG.12 $\varepsilon(\omega)$ for camphor sulfonic acid doped polyaniline metallic samples with conductivities in the order of $\sigma_A > \sigma_B > \sigma_C > \sigma_D$. Inset: σ_{dc} (T) for sample A. (After Kohlman, R.S., Zibold, A., Tanner, D.B., Ihas, G.G., Ishiguro, T., Min,Y.G., Mac Diarmid, A.G., and Epstein, A.J., *Phys. Rev. Lett*., 78, 3915, 1997. With permission.)

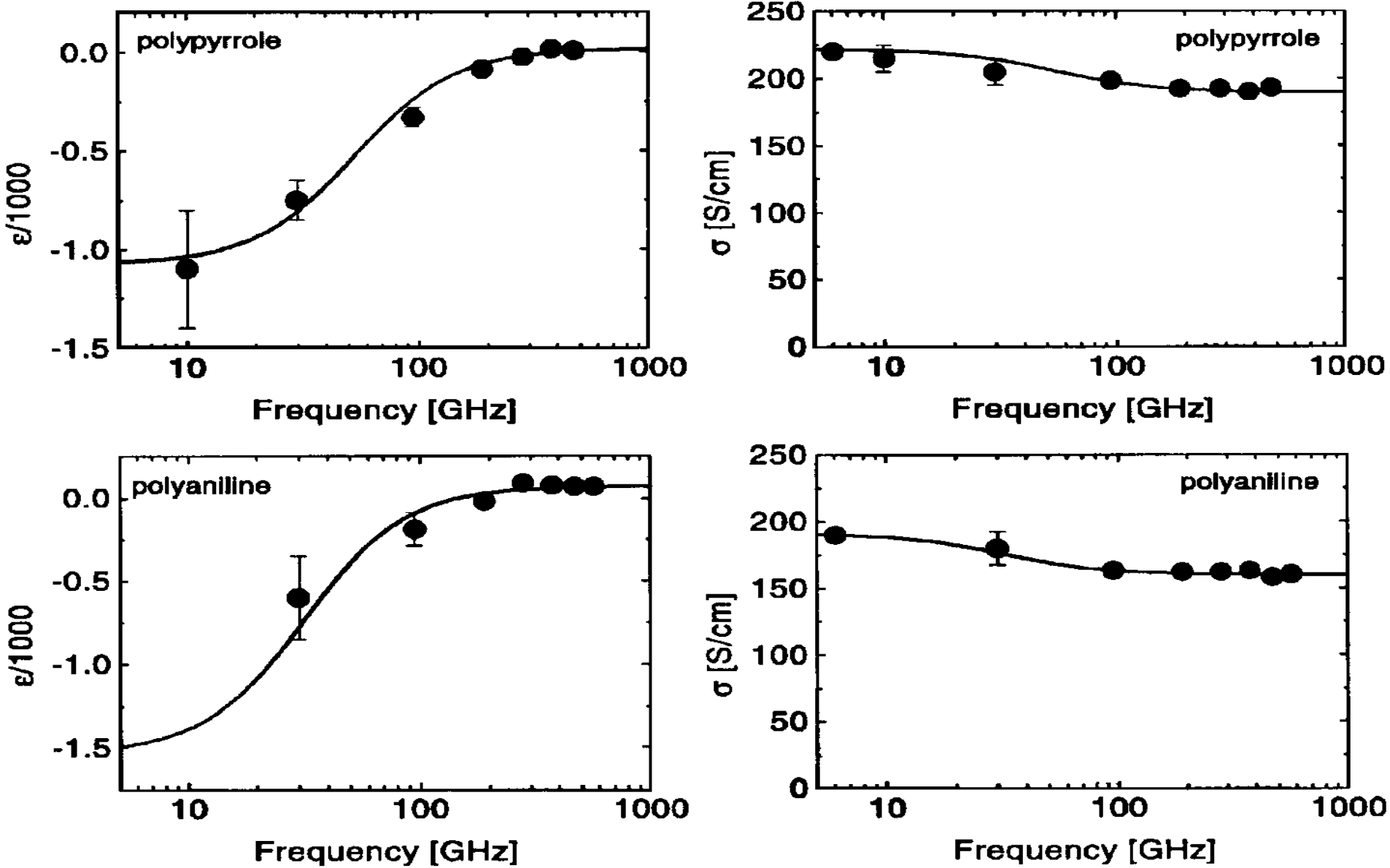

FIG.13 $\varepsilon(\omega)$ and $\sigma(\omega)$ for metallic-doped polymers. (From Martens, H.C.F., Reedijak, J.A., Brom, H.B., de Leuw, D.M., and Menon, R., *Phys. Rev. B* 63, 073203, 2001. With permission.)

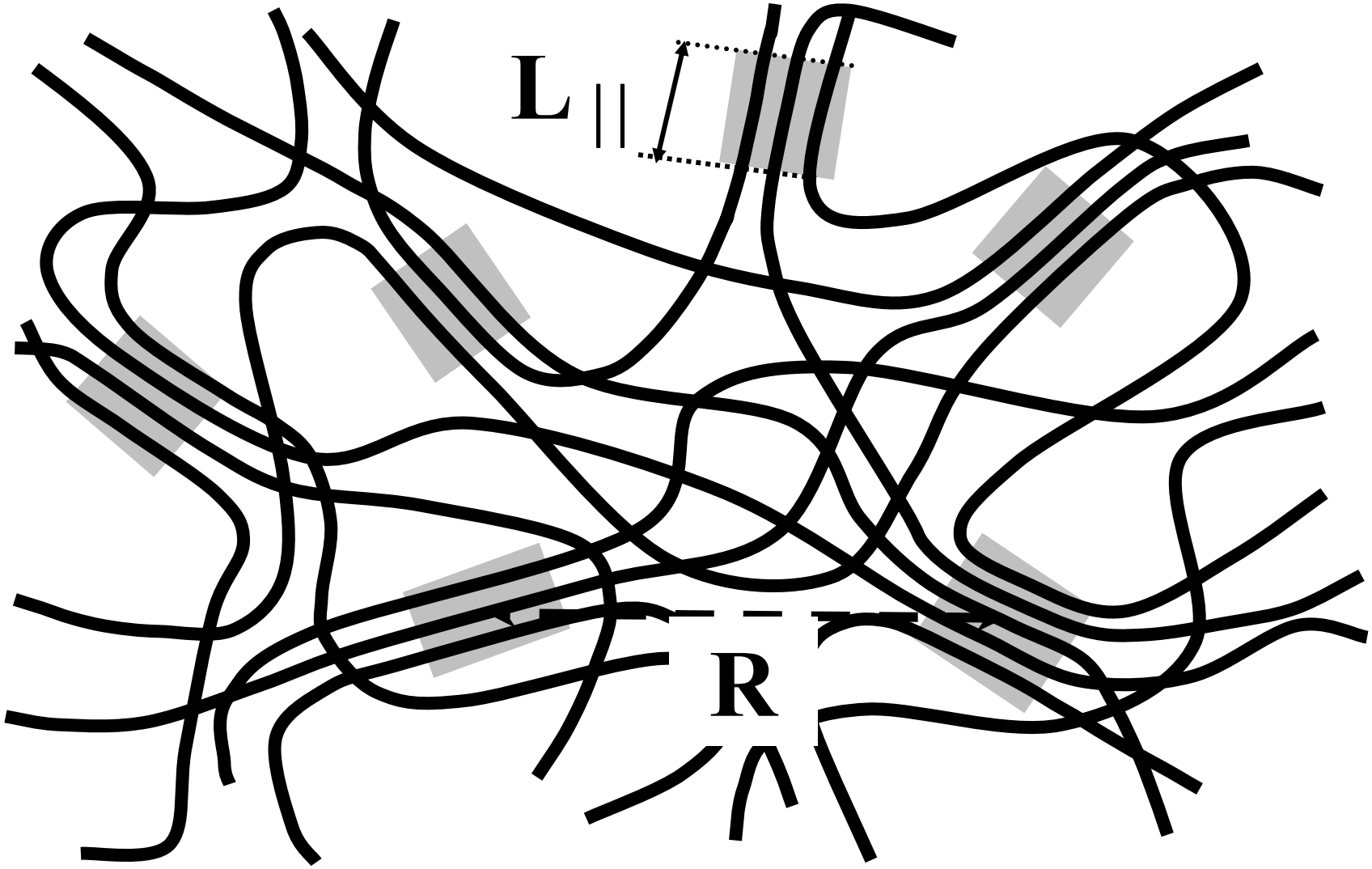

FIG.14 Schematic view on structure of polyaniline and polypyrrole. The lines represent polymer chains. The dashed squares mark the regions where polymer chains demonstrate the crystalline order. (After Prigodin, V.N. and Epstein, A.J., *Europhys. Lett*. 60, 750, 2002.With permission.)

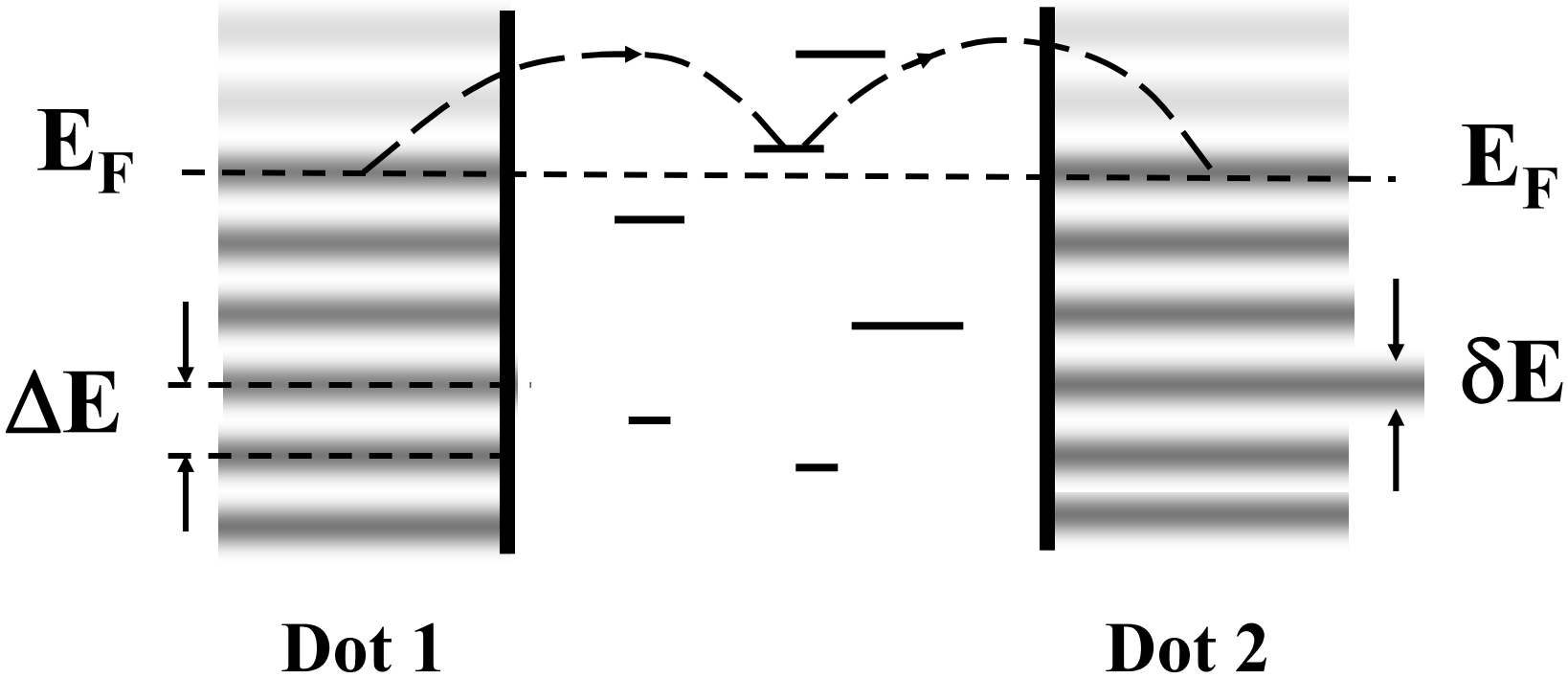

FIG.15 The electrical coupling between metallic grains is provided by resonance tunneling through localized states in the amorphous region. (After Prigodin, V.N. and Epstein, A.J., *Synth. Met*. 125, 43, 2002. With permission.)

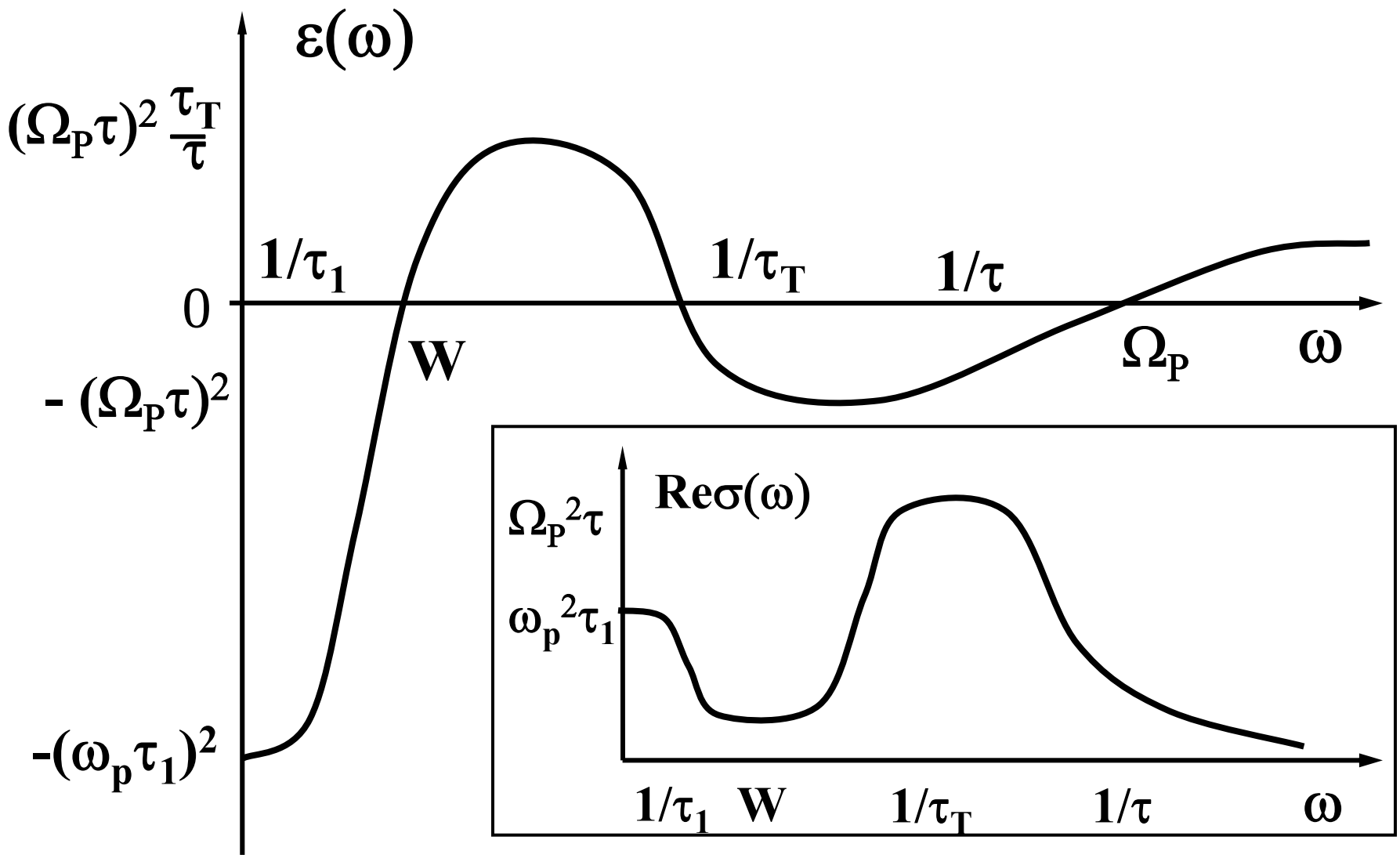

FIG.16 $\varepsilon(w)$ for the chain-linked granular model in the metallic phase. Inset: Re$\sigma(w)$. (After Prigodin, V.N. and Epstein, A.J., *Europhys. Lett*. 60, 750, 2002. With permission.)

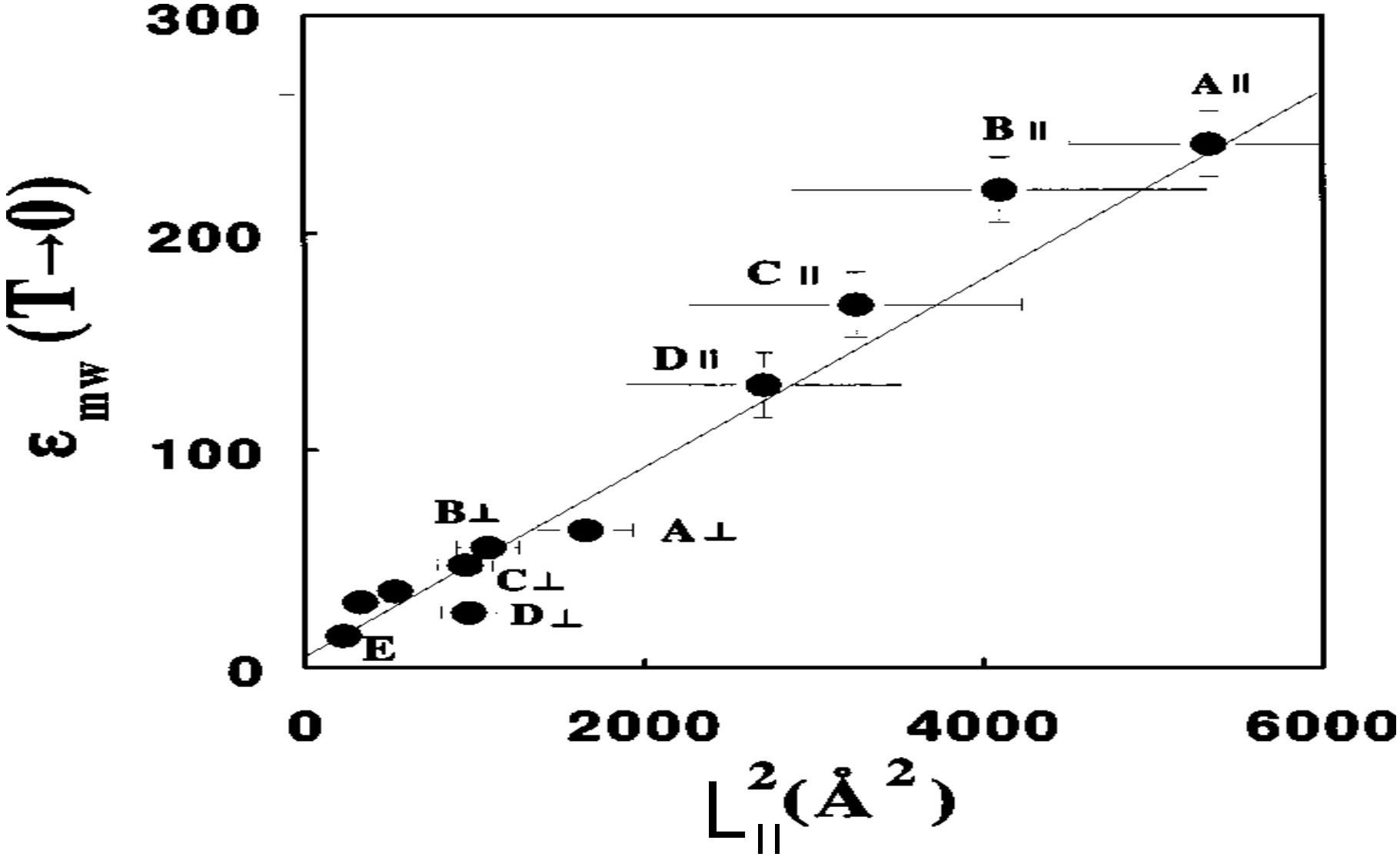

FIG.17 $\varepsilon_{mw}(T \rightarrow 0)$ vs. the square of crystalline coherence length $L^2_{||}$ for various polyaniline samples. (After Joo, J., Long, S.M., Pouget, J.P., Oh, E.J., MacDiarmid, A.G., and Epstein, A.J., *Phys. Rev. B* 57, 9567, 1998. With permission.)

CRC Press, 2008. ISBN-10: 0849392845

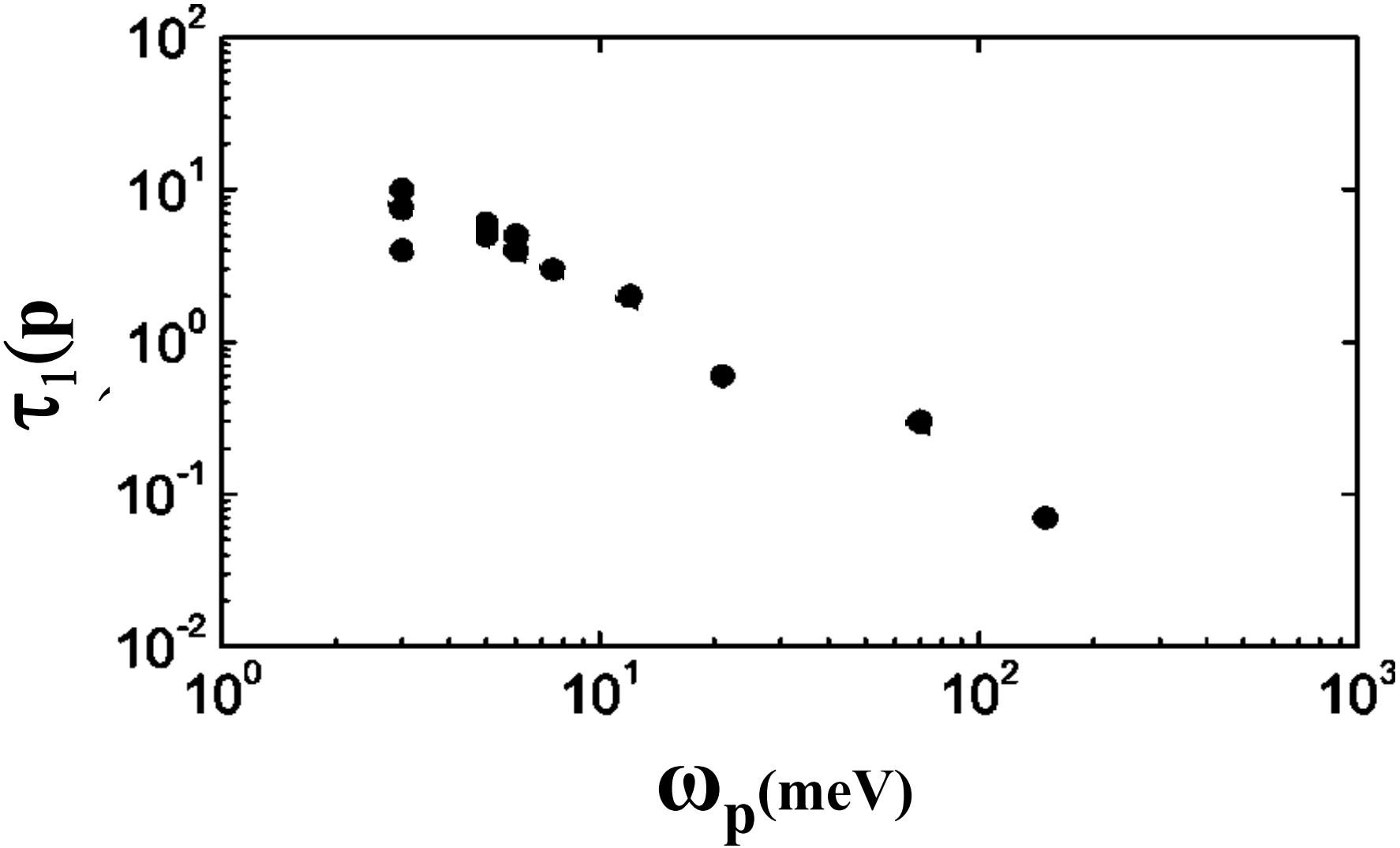

FIG.18 Experimental correlation between low-frequency relaxation time τ_1 (intergrain tunneling time) and low plasma frequency ω_p (intergrain hopping frequency). (From Martens, H.C.F., and Brom, H.B., *Phys. Rev. B* 70, 241201-1, 2004. With permission.)

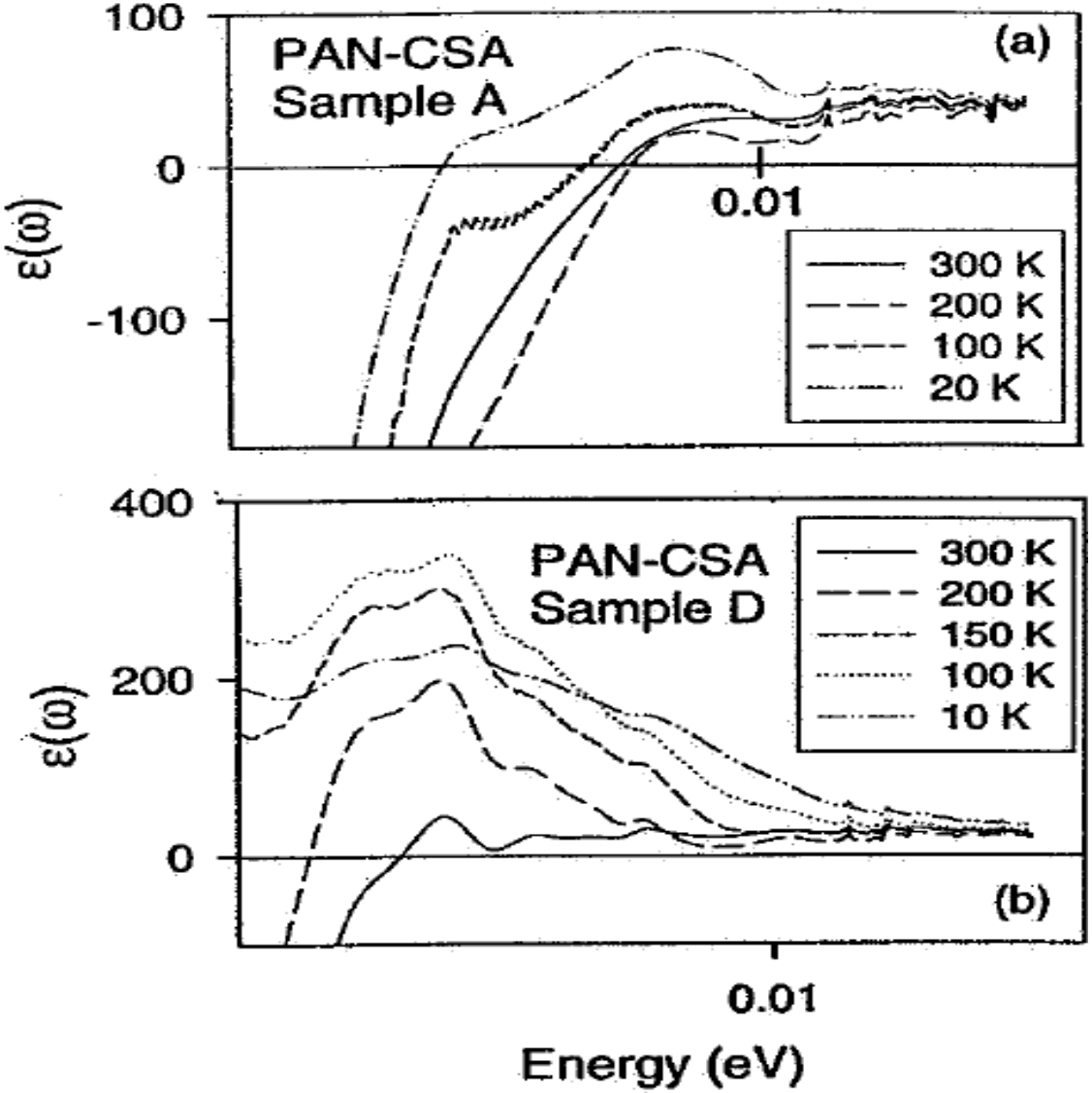

FIG.19 Dielectric response $\varepsilon(w)$ for (a) metallic PAN-CSA sample A and (b) insulating PAN-CSA sample D. The value of abscissa at the left hand axis is 0.002 eV. (From After Kohlman, R.S. and Epstein, A.J. *Handbook of Conducting Polymers*, 2nd edition, T.A. Skotheim, R.L. Elsenbaumer, J.R. Reynolds (eds.), Marcel Dekker, New York, 1998, With permission.)

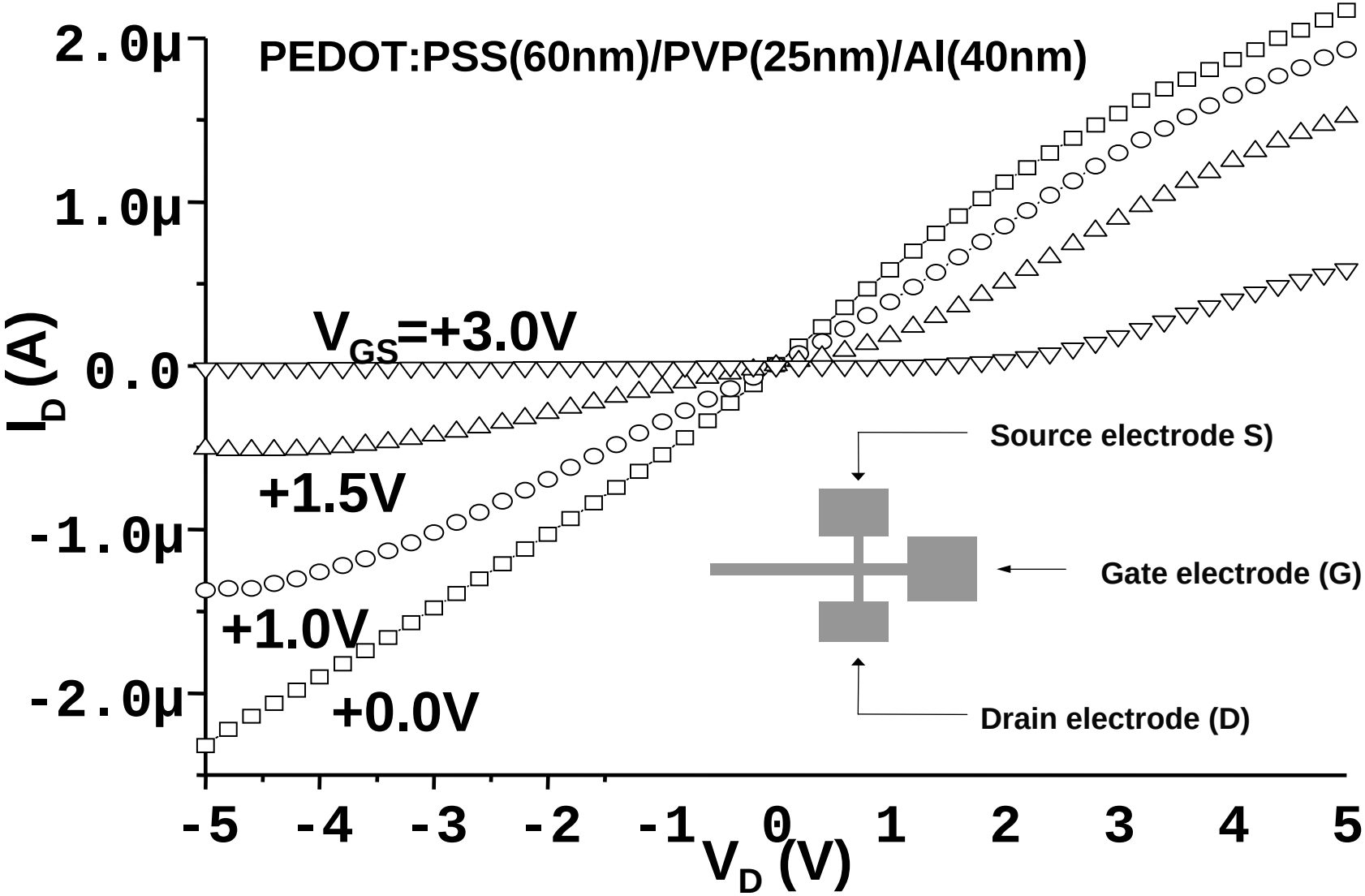

FIG.20 The drain–source current as the function of drain voltage of a thin active channel PEDOT:PSS/PVP film. (After F.-C. Hsu, V.N. Prigodin, and A.J. Epstein, *Phys Rev. B* 74, 235219, 2006. With permission.) Note PEDOT = poly(ethelenedioxytheophene), the dielectric layer is PVP (PVP = poly(inylphenol)).

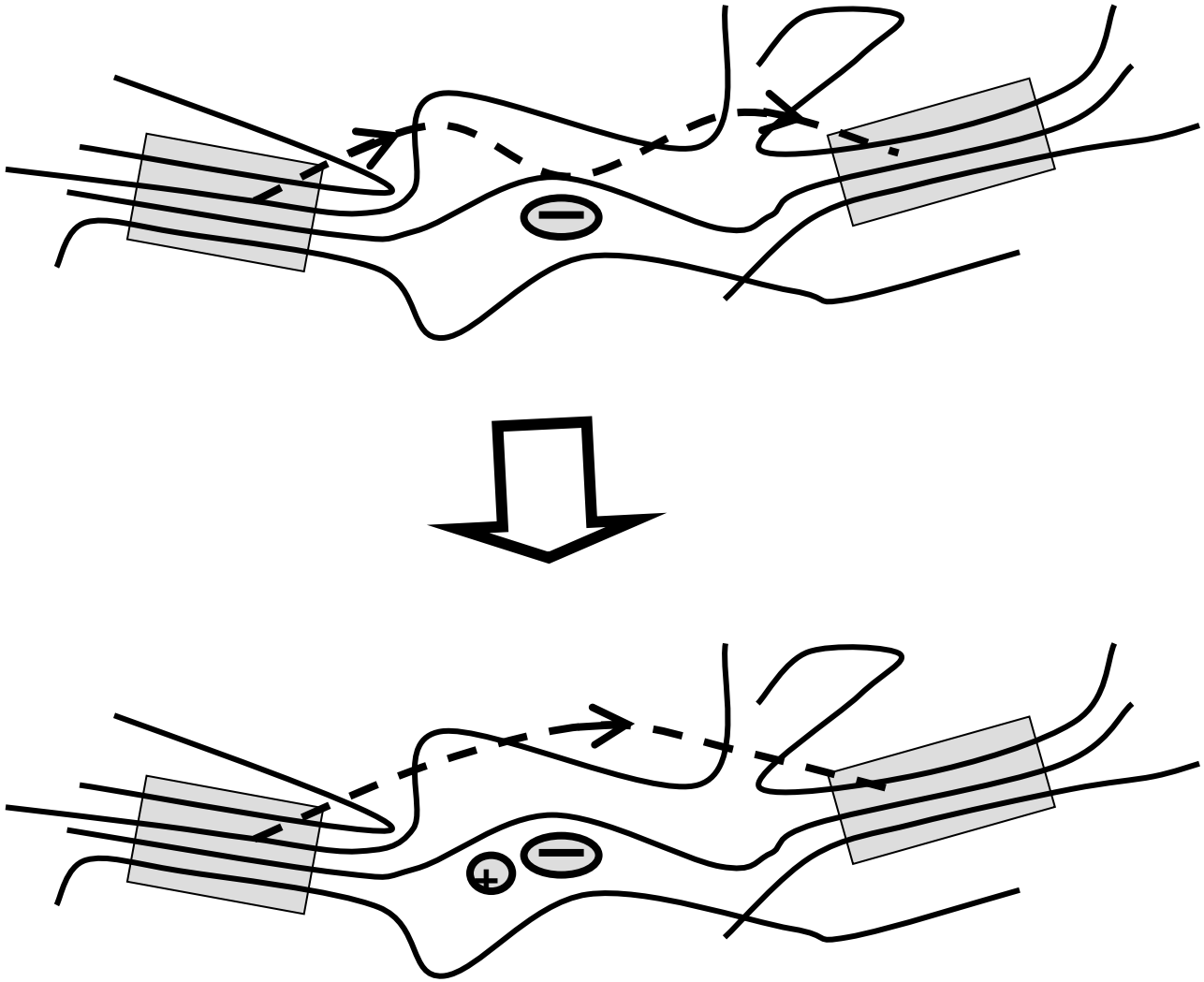

FIG.21 Ionic suppression of intergrain hopping. The compensation by cations of negative charge of acceptors removes the nearby localized state that provides for holes easy hopping between grains.

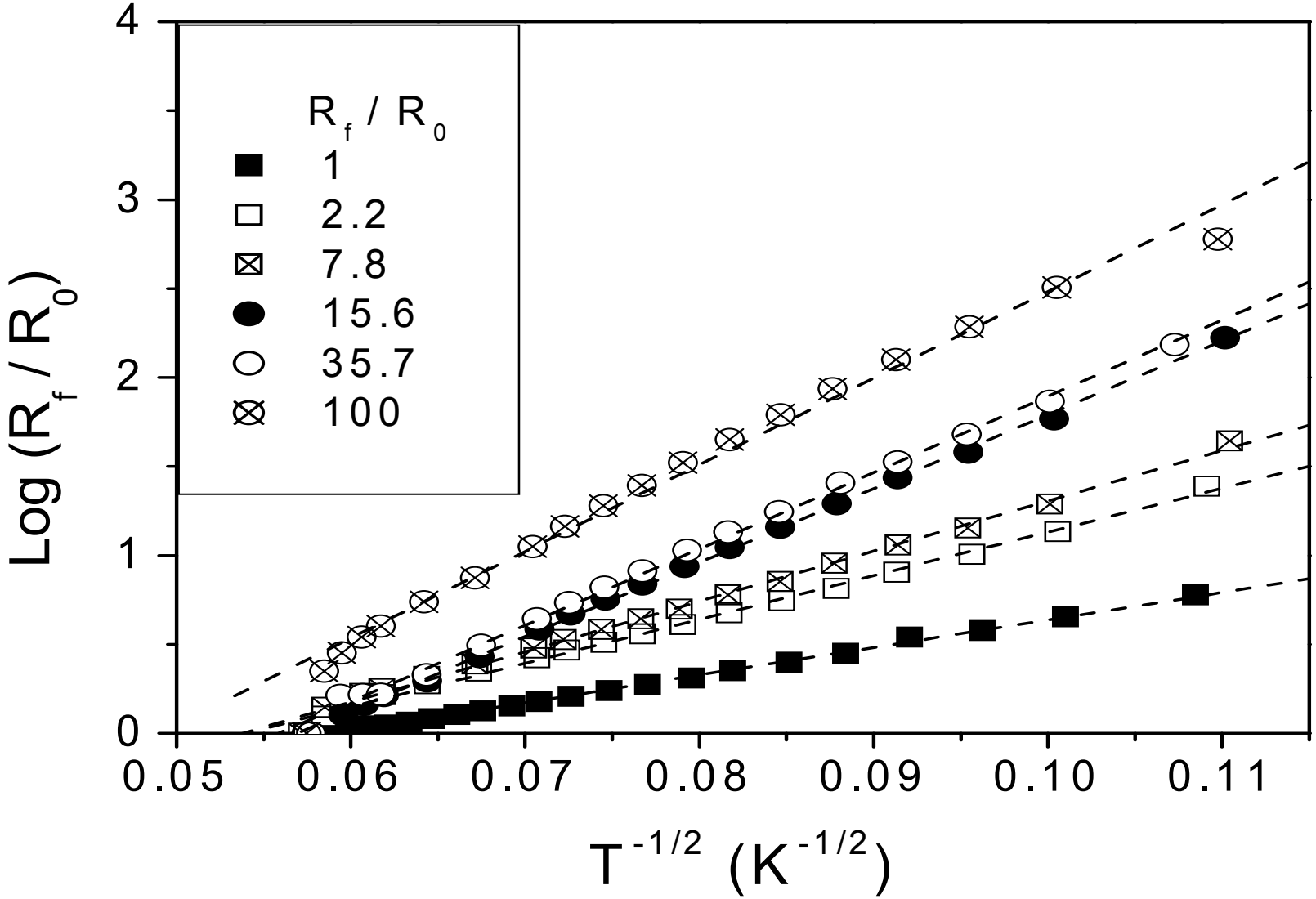

FIG.22 Quasi-1D Mott's law fit for temperature-dependent resistance at different conducting states R_f / R_0 induced by gate voltage applied at room temperature. (After F.-C. Hsu, V.N. Prigodin, and A.J. Epstein, *Phys Rev. B* 74, 235219, 2006. With permission.)